Pulse Repetition Frequency Multiplication With Spectral Selection in Fabry–Perot Filters

Konstantinos Yiannopoulos, Konstantinos Vyrsokinos, Dimitris Tsiokos, Efstratios Kehayas, N. Pleros, George Theophilopoulos, *Member, IEEE*, Thanassis Houbavlis, George Guekos, *Member, IEEE*, and Hercules Avramopoulos, *Member, IEEE*

***Abstract*—We present methods for obtaining high-repetition-rate full duty-cycle RZ optical pulse trains from lower rate laser sources. These methods exploit the memory properties of the Fabry–Perot filter for rate multiplication, while amplitude equalization in the output pulse train is achieved with a semiconductor optical amplifier or with a second transit through the Fabry–Perot filter. We apply these concepts to experimentally demonstrate rate quadruplication from 10 to 40 GHz and discuss the possibility of taking advantage of the proposed methods to achieve repetition rates up to 160 GHz.**

***Index Terms*—Fabry–Perot resonators, optical transmitters, semiconductor optical amplifiers.**

I. Introduction

THE expectation that new broad-band services will become available and useful for the end user has driven optical fiber telecommunications equipment manufacturers and, more generally, the research community to focus on the development of concepts to improve the data throughput in optical fiber network systems, and increasing the transmission capacity of optical fiber has been one of the key research themes. As such, repetition-rate upgrade of experiments is a universal and recurring step in the development process which is, however, associated with expense in terms of time and cost. A major contribution to this expense is related to the replacement of laser sources and their microwave drivers and amplifiers. This difficulty becomes apparent for experiments that are performed at very high data rates and use the return-to-zero modulation (RZ) format, where the laser source must generate a high-repetition-rate pulse train before modulation with the data signal. In the case of wavelength division multiplexing (WDM) experiments, the upgrade expense increases dramatically since it scales directly with the number of channels to be employed. Due to this cost scaling, advanced, multichannel, WDM transmission and networking experiments at high repetition rates can only be performed in the very best endowed laboratories of the world. To address this difficulty, several techniques have been proposed in the past to optically multiply the repetition rate of laser sources so as not to require changes in the microwave driver circuits. These techniques have included rational harmonic mode locking of fiber lasers [1]–[8] including its application to a multiwavelength source [9]–[11], the temporal fractional Talbot effect [12]–[14], the utilization of arrayed waveguide gratings [15] or fiber Bragg grating [16], and the use of Fabry–Perot (FP) filters with a free spectral range (FSR) that equals the desired line rate [17]–[19]. Even though mode-locked fiber lasers have provided impressive results, they have been confined to laboratory uses primarily due to the environmental sensitivity that they display. The rate multiplication process through the temporal fractional Talbot effect does not work by suppression of the lower frequency components, and as such it relies critically on dispersion compensation of the transmission line. This may place substantial constraints by amplitude-modulated data signals in network environments where data-originating sources and destinations are dynamically changing and so is the distance of dispersion between them. Additionally, the temporal fractional Talbot effectt assisted by the cross-gain modulation of a CW signal in a semiconductor optical amplifier (SOA), is able to generate real, rate-multiplied, amplitude-modulated free pulse trains [14] and so comprises a useful solution that can be used in real transmission systems. Arrayed waveguide gratings (AWGs) can also produce bursts of pulses at extremely high repetition rates, reaching 1 THz, but the multiplied pulses suffer from severe amplitude modulation and each burst of pulses lies at different wavelength. Fiber Bragg gratings can be used to emulate the transmission function of the FP filters, and they are an alternative technique which offers the advantage of simple writing on a fiber without high positioning accuracy. Rate multiplication with FP filters has the advantage of simplicity and robustness since commercially available FP filters may be used. However, unless the FP filter used has very high finesse and/or the rate multiplication factor is low, this technique results in periodically amplitude-modulated pulse trains. High-finesse FP filters have narrow bandwidth and consequently require fine matching with the repetition frequency of the initial pulse train.

In this work, we describe and demonstrate two techniques for the deployment of rate multiplication using FP filters of modest finesse that result in, practically, amplitude-modulation-free RZ pulse trains. The first method uses a modest finesse FP filter, which is followed by an SOA operated under heavy saturation and takes advantage of the amplitude equalizing properties of the SOA. The experimentally demonstrated circuit achieved a repetition rate multiplication from 10 to 40 GHz with a resulting amplitude modulation of 0.25 dB and a timing jitter of about

Manuscript received July 22, 2003; revised November 3, 2003.

K. Yiannopoulos, K. Vyrsokinos, D. Tsiokos, E. Kehayas, N. Pleros, G. Theophilopoulos, T. Houbavlis, and H. Avramopoulos are with the Department of Electrical and Computer Engineering, National Technical University of Athens, Zografou, GR 15773 Athens, Greece (e-mail: kyianno@cc.ece.ntua.gr).

G. Guekos is with the Swiss Federal Institute of Technology Zurich, ETH Hoenggerberg, CH-80923 Zurich, Switzerland.

Digital Object Identifier 10.1109/JQE.2003.821534

650 fs. The second technique uses only a single FP filter of modest finesse, used in a double-pass arrangement to extend its lifetime and to produce modulation-free pulse trains. This circuit achieved a four-time rate multiplication factor and resulted in pulse trains with 0.12-dB amplitude modulation and 500-fs timing jitter, equal to the timing jitter of the original gain-switched diode.

Both configurations are simple to implement and cost-effective and proved ultrastable under laboratory conditions, since they could run for many hours without any adjustments. Additionally they can be used to simultaneously upgrade the repetition rate of several low-rate RZ-pulsed laser sources at different wavelengths without the need for any high-speed electronics, dividing thus the total cost of the circuit to many channels.

The rest of the paper is arranged in two main sections, each presenting the corresponding rate-multiplication technique. The principle of operation and the experimental implementation are presented along with the experimental results for both circuits. Furthermore, the underlying theory for each technique is described in detail, and the theoretical results are discussed toward the extension to higher rates.

II. Rate Multiplication With FP Filters and SOAs

A. Principle of Operation and Experimental Implementation

Rate multiplication with Fabry–Perot filters that have an FSR equal to a multiple integer of the initial rate of the laser source and equal to the desired final rate has been reported previously [17]–[19]. The method relies on the property of an FP filter that its time-domain impulse response is an exponentially decaying sequence of pulses at a repetition frequency equal to its FSR and whose decay constant is determined by the filter finesse (F). Equivalently, in the frequency domain, the initial RZ pulse train has harmonics at multiple integers of its repetition rate and the FP filter allows only those harmonics present within its resonant peaks to be transmitted. The degree of suppression of the unwanted harmonics is determined by the finesse of the FP filter, and, for lower finesse FP filters or high multiplication factors, this suppression is only partial, resulting in an amplitude-modulated pulse train. Use of very high-finesse FP filters is not desirable because their sharp resonance peaks result in very narrow ranges of frequency operation, they incur higher power losses and will lead to loss of coherent addition in the filter for pulses temporally delayed beyond the coherence time of the initial signal. For rate multiplication, it is therefore desirable to use low-finesse FP filters, but arranged so as not to compromise the quality of the pulse train in terms of amplitude modulation. In this section, we show that use of an SOA operated in heavy saturation following the FP filter can produce nearly modulation-free pulses. For an SOA operated in heavy saturation, pulses with high energy receive less gain than pulses with lower energy so that deviations of their amplitude at the output of the amplifier are minimized. Even so, a single pass through the amplifier is not enough to suppress fully the amplitude modulation from the FP filter. It was found however, that reintroduction of this pulse train into the SOA for a second time can result in nearly complete amplitude modulation elimination. This concept was utilized for four-times rate multiplication from 10 to 40 GHz.

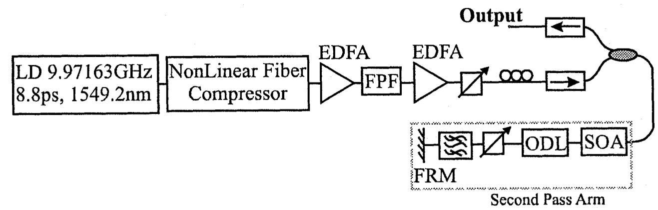

Fig. 1. Experimental setup. ODL: optical delay line; FRM: Faraday rotator mirror.

The experimental setup is depicted in Fig. 1. The initial lower rate pulse train was produced by a gain-switched DFB laser operating at 1549.2 nm. The laser yielded 8.8-ps pulses at a repetition rate of 9.97 GHz, after linear compression through dispersion compensation fiber (DCF) with total negative dispersion of 54.27 ps/nm. The laser output pulses were then amplified in an erbium-doped fiber amplifier (EDFA) and had their temporal width reduced in a two-stage nonlinear fiber compressor comprised of alternating sections of DCF and single-mode fiber. By filtering the compressor output with a 2-nm filter, 3.2-ps nearly transform-limited hyperbolic secant pulses were obtained. The pulse train was further amplified and fed into the FP filter. The FP filter was an AR-coated fused quartz substrate with an FSR equal to 39.88 GHz and a finesse of 50. The FP filter partially suppresses the 10-, 20-, and 30-GHz harmonics while leaving the 40-GHz component unattenuated. After exiting from the FP filter, the signal was re-amplified and inserted into a 3-dB coupler used for monitoring and to provide the output of the source on its return path from the SOA amplitude equalization stage. Following the 3-dB coupler, the signal was introduced into a commercially available 1.5-mm-long SOA that exhibited a small-signal gain of 24 dB at 1549.2 nm, 3-dB polarization gain dependence, 10%-90% gain recovery time of 65 ps, and 10-fJ saturation energy, when driven at a 700-mA dc current. After passing once through the SOA, the pulse train entered the second pass arrangement where it was filtered in a 2.8-nm band-pass filter and was reflected back again into the SOA by a Faraday rotator mirror (FRM). In order to further reduce the amplitude modulation after the second pass, it was found that for best operation two conditions must be met.

1) The energy of the second pass pulses should be significantly lower, so as the first pass pulses dominate the gain dynamics of the amplifier. In this case the pulses coming from the feedback arm provide a small correction, which is time dependent, in the gain of the SOA.
2) To exploit this time dependency, optimum operation of the circuit can be achieved by nearly synchronizing in the SOA the counter-propagating pulse trains, so that the highest energy pulses from each pulse train transit the SOA at the same time.

To fulfill these conditions, variable optical attenuators were used at the two ports of the SOA and temporal synchronization between the counterpropagating pusle trains was achieved with a variable optical delay line (ODL).

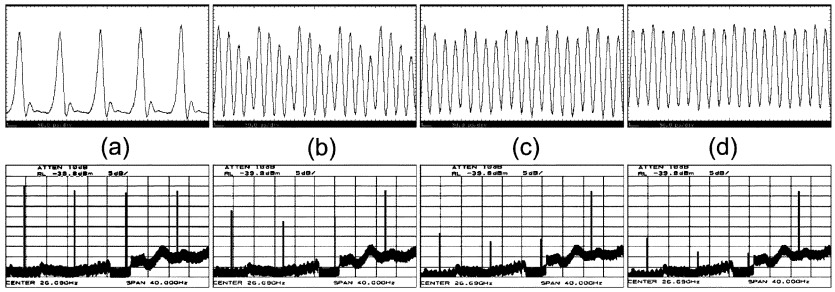

Fig. 2. Oscilloscope traces and corresponding RF spectra at the (a) compressor output, (b) Fabry–Perot filter output, (c) output after first SOA pass, and (d) output after second SOA pass. Oscilloscope trace time base is 50 ps/div. Microwave spectra amplitude scale is 5 dB/div and frequency scale is 4 GHz/div.

B. Experimental Results

Fig. 2 shows the experimental results obtained using a 40-GHz sampling oscilloscope and a 50-GHz microwave spectrum analyzer. Fig. 2(a) illustrates the oscilloscope trace and the corresponding microwave spectrum of the initial 10-GHz clock signal. Fig. 2(b) displays the signal at the output of the FP filter, showing a 40-GHz clock pulse train with 1.65-dB amplitude modulation. Fig. 2(c) and (d) depicts the pulse trains after the first and second passes through the SOA and show that the amplitude modulation reduces to 0.8 and 0.15 dB, respectively, as seen on the sampling oscilloscope. The microwave spectrum of the pulse train after the second pass through the SOA shows suppression in excess of 26 dB for the 10-GHz component while the 20- and 30-GHz frequency components are suppressed by approximately 35 dB. Analysis of this spectrum with inverse Fourier series indicates that the amplitude modulation of the signal is below 0.25 dB, which is in close agreement to the measurements made with the sampling oscilloscope. Spectral analysis shows also that the timing jitter is less than 650 fs. Adjustment of the optical power and relative timing of the signals for the two passes in the SOA is required in order to obtain the results shown in Fig. 2(d). The input powers of the pulse trains before entering the SOA were 850 μW for the first pass and 80 μW for the second pass, corresponding to average energies per pulse of 25 and 2 fJ, respectively. With these powers, the SOA is operated under deep saturation and the degree of saturation is primarily determined by the first pass signal. By arranging the temporal adjustment of the second pass signal with respect to the first pass using the ODL, it is possible to enhance the amplitude equalization properties of the SOA for the second pass pulse train. For the best performance, the second pass pulses had to enter the SOA delayed by approximately 5 ps with respect to their equivalent from the first pass.

Fig. 3 shows the autocorrelation trace and optical spectrum of the output pulse train. Assuming a hyperbolic squared-secant profile, the output pulses have a full-width at half-maximum (FWHM) of 3.8 ps. This is marginally increased from 3.5 ps at the input of the SOA primarily due to birefringence of the SOA and polarization dependence of its gain. The 3-dB bandwidth of the optical spectrum was 90 GHz and the resulting time–bandwidth product was 0.342, which is in close agreement to the value for a hyperbolic squared-secant profile. The output power of the source was 680 μW. The arrangement was found to be stable in time and the characteristics of the output pulses would remain unchanged without requiring adjustment for many hours.

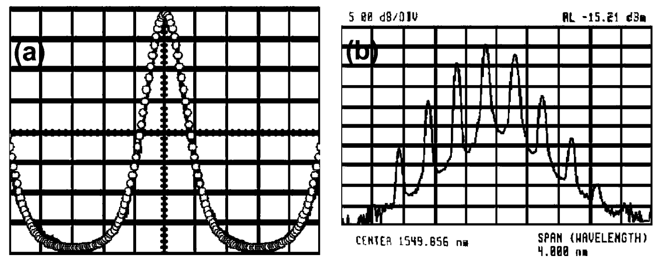

Fig. 3. (a) Second-harmonic autocorrelation trace. The white dots indicate the fitted hyperbolic secant periodic autocorrelation profile. The time base is 2.74 ps/div. (b) Optical spectrum trace. The amplitude scale is 5 dB/div and the frequency scale is 0.4 nm/div. The resolution 0.08 nm.

C. Theory of the Principle and Extension to Higher Rates

A simulation tool was developed to investigate the optimization of the proposed rate-multiplication scheme and the feasibility of extending its operation to higher rates, up to 160 GHz. The FP filter is described both in the time and frequency domains by analytical expressions. The impulse response function of a single FP filter with mirror reflectivity R is given by the following sum:

$$h(t) = (1-R) \cdot \sum_{n=o}^{\infty} R^n \cdot \delta\left(t - \frac{n}{\mathrm{FSR}}\right). \tag{1}$$

In order to achieve k-times rate multiplication, the sum over the series of overlapping pulses at time intervals equal to multiples of FSR^{-1}, when the output reaches the steady state, must be calculated. Provided that the pulse duration is very short compared to the inverse FSR, the power of the nth pulse inside the period of the pulse series can be expressed as

$$\begin{aligned} x_n &= (1-R)^2 \cdot R^{2(n-1)} \cdot \sum_{i=o}^{\infty} \left(R^{2k}\right)^i = \\ &= \frac{(1-R)^2}{1-R^{2k}} \cdot R^{2(n-1)},\ n = 1, 2, \ldots, k. \end{aligned} \tag{2}$$

Therefore, k-times rate multiplication imposes an amplitude modulation of

$$AM_{\mathrm{sp}}(\mathrm{dB}) = 10 \cdot \log\left[\frac{\min(x_n)}{\max(x_n)}\right] = 10 \cdot \log(R^{2(k-1)}). \tag{3}$$

The time dependence of the SOA gain saturation and its recovery for picosecond pulses is described by the equations in

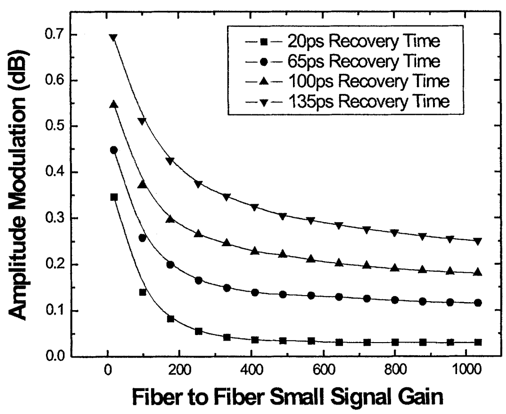

Fig. 4. Amplitude modulation versus SOA small-signal gain for various recovery times.

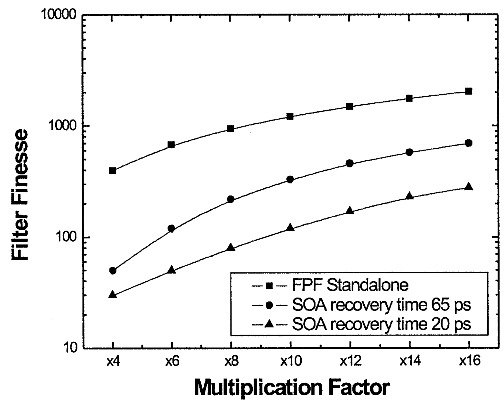

Fig. 5. Calculated filter finesse versus desirable pulse repetition frequency under the constraint that amplitude modulation remains close to 0.2 dB, for SOAs with recovery time equal to 20 ps, 65 ps, or no SOA.

TABLE I
SIMULATION VALUES

	Parameter	Value
Optical Signals	Pulsewidth	3.5ps
	Input Power	850 μW
	Feedback Power	80 μW
Fabry-Perot Filter	Finesse	50
Optical Amplifier	Saturation Energy	10fJ
	Recovery Time	Variable
	Small Signal Gain	Variable

TABLE II
SIMULATION VALUES

	Parameter	Value
Optical Signals	Pulsewidth	Variable
	Input Power	850 μW
	Feedback Power	80 μW
Fabry-Perot Filter	Finesse	Variable
Optical Amplifier	Saturation Energy	10fJ
	Recovery Time	Variable
	Small Signal Gain	24dB

[20], and these were modified to take into account that the signal transits the amplifier twice. Assuming an amplitude modulation of 1.65 dB for the pulse train at the output of the FP filter and a small-signal gain of 24 dB and 65-ps gain recovery time for the SOA, the simulated output pulses have 0.17-dB amplitude modulation. This theoretical result is very close to the experimentally obtained value of 0.25 dB from the microwave spectrum at the output of the source. The optimization performed with the aid of this simulation tool is depicted in Fig. 4, where the amplitude modulation has been plotted as a function of the small-signal gain of the amplifier for four sets of recovery times. The parameters for the simulation were derived from the experimental setup and are depicted in Table I.

The curves indicate that the amplitude modulation decreases rapidly as the small-signal gain of the SOA increases and beyond a value of approximately 23 dB remains constant to a value defined by the recovery time. Small variations of the gain parameter within this regime cause no significant changes to the amplitude modulation. On the other hand, the crucial parameter which significantly contributes to the minimization of the amplitude modulation is the recovery time of the semiconductor. From Fig. 4, it is apparent that a SOA with a 20-ps recovery time and 20-dB gain can reduce the amplitude modulation to less than 0.1 dB. Therefore, low amplitude modulation (less than 0.15 dB) can be achieved either using conventional SOAs with fast recovery time (65 ps) that can provide a small-signal gain that exceeds 23 dB or SOAs with very fast recovery times (20 ps) and small-signal gain less than 20 dB as quantum dot SOAs [21], [22] or SOAs with reduced recovery time by optical pumping [23] or beam holding [24].

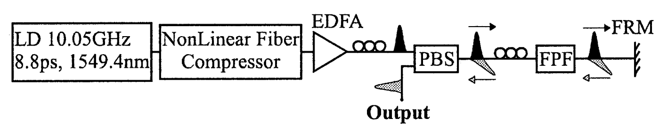

Fig. 6. Experimental setup. PBS: polarization beam splitter; FRM: Faraday rotator mirror.

Furthermore, these devices could be utilized to achieve higher rates up to 160 GHz and this is shown in Fig. 5, which was obtained using the simulation values summarized in Table II. Fig. 5 shows the required filter finesse so that the output pulse train achieves a given rate-multiplication factor with amplitude modulation equal to 0.2 dB for SOAs with different recovery times. In order to achieve a 16-times multiplication factor to produce 160-GHz pulse trains, a stand-alone FP filter of an impractically high finesse of 2000 is required. If, however, a regular SOA with 65-ps recovery time is used, an FP filter with a finesse of 800 is needed, and if an SOA with 20-ps recovery time is available, then an FP filter with a finesse of 280 can ensure multiplication to 160 GHz with 0.2-dB modulation. Given that FP filters can operate over broad wavelength ranges and that SOAs have broad amplification spectra, this method can, in principle, be extended to multiply the repetition rate of several laser sources simultaneously.

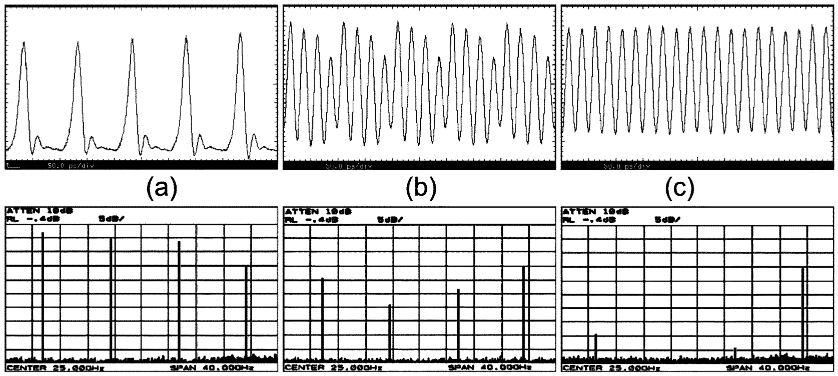

Fig. 7. Oscilloscope traces and corresponding microwave spectra (a) at the compressor output, (b) after the first pass through the FP filter, and (c) after the second pass through the FP filter. The oscilloscope trace time base is 50 ps/div. The microwave spectra amplitude scale is 5 dB/div and the frequency scale is 4 GHz/div.

III. Rate Multiplication With a Single Fabry–Perot Filter

A. *Principle of Operation and Experimental Implementation*

In this section, we show an alternative method to achieve modulation-free repetition-rate multiplication of a low-rate RZ laser source using a single FP filter. This technique requires the application of the multiplication transfer function of the FP filter, consecutively, twice, as if two identical FP filters are cascaded. In this way, the rate-multiplied and amplitude-modulated output from the first is used as the input to the second. In order to avoid the use of two filters, the output from the filter may be re-introduced in a counter direction by the use of an FRM instead. The double pass through the filter modifies its time-domain impulse response function so that it is no longer the regular decaying tail, but consists of a fast rising edge and a slow decaying tail with an enhanced $1/e$ lifetime. In the frequency domain, the transfer function of the filter is also modified and its resonance peaks become sharper, thus resulting in an enhanced nominal finesse and greater suppression of out-of-band spectral components while its bandwidth is reduced to about half. These attractive features of the double-pass configuration lead to lower amplitude modulation when a multiplication rate process is realized, in comparison with the single-pass case.

This technique has been applied to a four-times line rate multiplication from 10 to 40 GHz. Fig. 6 shows the experimental setup. The initial pulse train was produced from a gain-switched DFB laser at 1549.4 nm. The laser diode operated at 10.05 GHz and produced 8.8-ps pulses after linear compression in a DCF fiber of total negative dispersion of 55.58 ps/nm. This pulse train was amplified, driven to the two-stage nonlinear fiber compressor, and then again amplified and fed into the FP filter through the ordinary axis of a fiber polarization beam splitter (PBS) so that only a single state of polarization entered the double-pass arm. The FP filter was an AR-coated fused quartz substrate with an FSR equal to 40.2 GHz and a finesse of 50. For optimum performance, the polarization state of the incident beam was adjusted with a polarization controller before the FP filter. At its output, an FRM was used to reflect the rate-multiplied pulse train back into the FP filter. Finally, the output of the setup was obtained at the extraordinary axis of the PBS due to the 90° polarization rotation at the FRM.

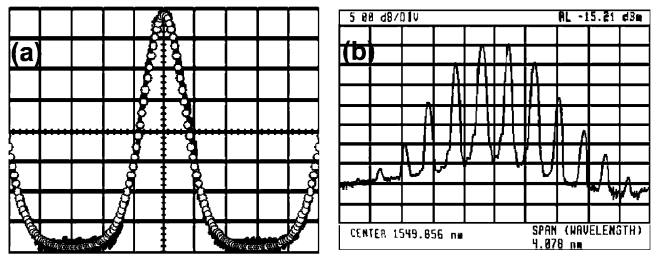

Fig. 8. (a) Second-harmonic autocorrelation trace. The white dots indicate the fitted hyperbolic secant periodic autocorrelation profile. Time base is 2.74 ps/div. (b) Optical spectrum trace. The amplitude scale is 5 dB/div and the frequency scale is 0.4 nm/div. Resolution 0.08 nm.

B. *Experimental Results*

The performance of the source was evaluated with a 40-GHz sampling oscilloscope and a 50-GHz microwave spectrum analyzer. Fig. 7(a) illustrates the oscilloscope trace and the corresponding microwave spectrum of the initial 10.05-GHz signal. Fig. 7(b) displays the signal after its first pass through the FP filter and shows the 40.2-GHz pulse train with amplitude modulation 1.65 dB as recorded on the sampling oscilloscope. Fig. 7(c) shows the pulse train after its second pass through the FP filter, and its amplitude modulation is now reduced to 0.11 dB. The corresponding microwave spectra reveal that double passing through the FP filter results in the suppression of the 20-GHz component in excess of 47 dB, while the 10- and 30-GHz components are suppressed by approximately 40 dB. Inverse Fourier analysis of the microwave spectrum of the output pulse train indicates that, with this harmonic suppression, the amplitude modulation of the signal is below 0.12 dB, and this value compares very well with the amplitude modulation measured with the sampling oscilloscope. Spectral analysis has also shown that the timing jitter of the rate-multiplied pulse train was less than 500 fs, and this was found to be equal to the timing jitter of the gain-switched diode pulse train. Fig. 8(a) and (b) shows the second-harmonic generation autocorrelation and optical spectrum of the 40-GHz pulse train, assuming a hyperbolic secant profile the output pulses have 3.2 ps and 100 GHz temporal and spectral widths (FWHM). These values yield a time–bandwidth product of

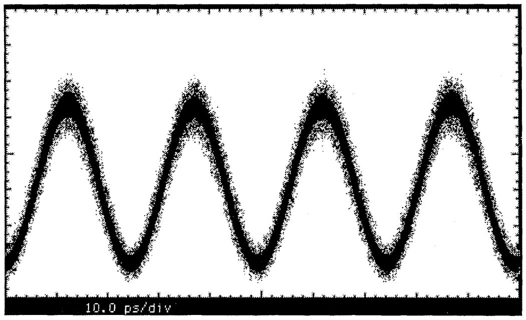

Fig. 9. Waveform of the output 40-GHz pulse train. The time base is 10 ps/div.

0.32, which is very close to the theoretically expected value for a hyperbolic squared-secant profile. Finally, Fig. 9 shows the 40.2-GHz pulse train on the sampling oscilloscope after clock recovery, indicating a clear, open-eye signal, which, using the oscilloscope's built-in-measurement suite, has a timing jitter of 500 fs. The pulse train was found to be stable in time under laboratory conditions. Even though the FP filter was a bulk device, the arrangement required only minimal re-adjustment from day-to-day for best performance for the duration of the experiment.

C. Theoretical Analysis and Extension to Higher Rates

The transfer function of a single-pass FP filter is

$$T_{\mathrm{sp}}(f)=\frac{1}{1+\left(\frac{2\cdot\sqrt{R}}{1-R}\cdot\sin\left(\frac{\pi\cdot f}{\mathrm{FSR}}\right)\right)^2} \tag{4}$$

and a double pass through the same filter yields

$$T_{\mathrm{dp}}(f)=\frac{1}{\left(1+\left(\frac{2\cdot\sqrt{R}}{1-R}\cdot\sin\left(\frac{\pi\cdot f}{\mathrm{FSR}}\right)\right)^2\right)^2}. \tag{5}$$

The bandwidth of the double-pass transfer function B_{dp} is related to the bandwidth of the single-pass transfer function B_{sp} by

$$\begin{aligned}B_{\mathrm{dp}}&=\frac{2\cdot\mathrm{FSR}}{\pi}\cdot\arcsin\left(\sqrt{\sqrt{2}-1}\cdot\sin\left(\frac{\pi\cdot B_{\mathrm{sp}}}{2\cdot\mathrm{FSR}}\right)\right)\\&\cong\sqrt{\sqrt{2}-1}\cdot B_{\mathrm{sp}}.\end{aligned} \tag{6}$$

The approximation normally holds, as finesse values are usually larger than 10. This relation shows that the double-pass through the FP filter results in a relatively small decrease in the bandwidth of the resonance peaks of the filter. Specifically, the double-pass FWHM bandwidth is $\sqrt{\sqrt{2}-1}$ or 64% of the FWHM bandwidth of the single pass. The single-pass FWHM bandwidth of the FP filter in our experiment was measured to be 800 MHz and its double-pass bandwidth was 510 MHz. The time-domain analysis provides analytical results for the double-pass impulse response function. This is derived by performing a double sum on the impulse response function (1) of the stand-alone FP filter. The resulting analytical expression is

$$h(t)=(1-R)^2\cdot\sum_{n=o}^{\infty}(n+1)\cdot R^n\cdot\delta\left(t-\frac{n}{\mathrm{FSR}}\right) \tag{7}$$

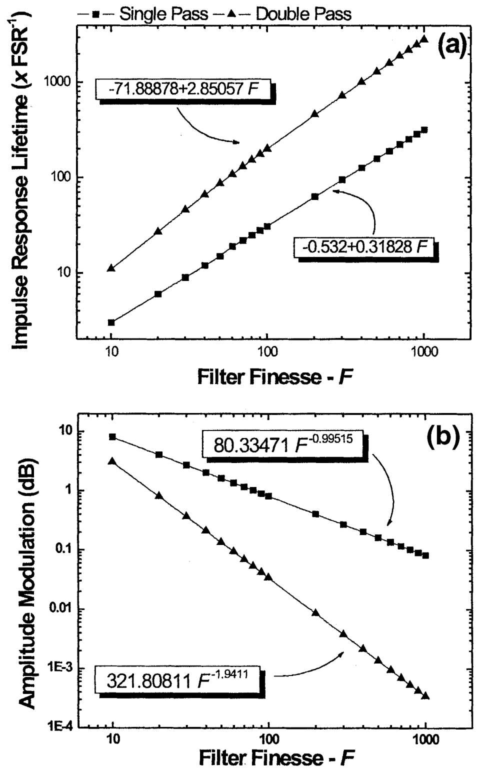

Fig. 10. (a) Calculated impulse response $1/e$ lifetime versus FP filter finesse. (b) Calculated amplitude modulation versus FP filter finesse, in the single and double pass cases.

and consequently the $1/e$ lifetime of the double-pass filter is $[m]/\mathrm{FSR}$, where m is the solution of the equation

$$(m+1)\cdot R^m=\frac{1}{e}. \tag{8}$$

Correspondingly, the single-pass $1/e$ lifetime is given by $[l]/\mathrm{FSR}$, where l is the solution of

$$R^l=\frac{1}{e}. \tag{9}$$

Equations (8) and (9) verify that $[m]>[l]$ and so the lifetime of the double-pass case is larger, explaining the lower amplitude modulation as far as repetition-rate multiplication is concerned, but the degree of enhancement can only be assessed after solving (8) and (9) numerically. The solutions of (8) and (9) are presented in Fig. 10(a), where the impulse response $1/e$ lifetime of the single- and double-pass cases, respectively, is plotted against the filter finesse. Double passing through the FP filter clearly improves the impulse response duration as compared to the single pass case, while the duration improvement ranges from three to nine times for finesses between 10 and 1000. The time domain analysis relies on the impulse response function of the double pass which is derived by taking the sum over the series of overlapping pulse at time intervals equal to multiples of FSR^{-1}, when the output reaches the steady state. If the pulse duration is very short compared to the inverse FSR, the power

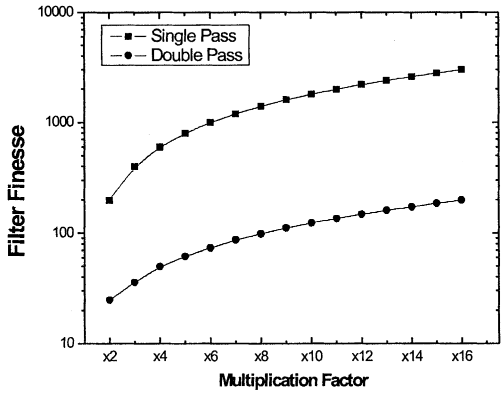

Fig. 11. Required filter finesse versus desirable pulse repetition frequency for the single- and double-pass cases under the constraint that amplitude modulation remains under 0.14 dB.

of the nth pulse inside the period of the pulse series, can be expressed as

$$x_n = (1-R)^4 \cdot R^{2(n-1)} \cdot \sum_{i=o}^{\infty} (k \cdot i + n) \cdot (R^{2k})^i = \left(\frac{(1-R)^2}{1-R^{2k}}\right)^2 \cdot R^{2(n-1)} \cdot \left((k-n) \cdot R^{2k} + n\right) \quad (10)$$

where $n = 1, \ldots, k$.

In this case, there is no simple relation for the amplitude modulation; however (3) is transformed to

$$AM_{dp}(\text{dB}) = 10 \cdot \log\left(\frac{\min(x_n)}{\max(x_n)}\right) = = 10 \cdot \log\left[\frac{\max(n)[R^{2\cdot(n-1)} \cdot ((k-n) \cdot R^{2k} + n)]}{\min(n)\left[R^{2\cdot(n-1)} \cdot ((k-n) \cdot R^{2k} + n)\right]}\right]. \quad (11)$$

For the sake of comparison, (10) and (11) are plotted versus the filter finesse in Fig. 10(b) for the specific case of $k = 4$, which is the multiplication process from 10 to 40 GHz. By curve fitting, the amplitude modulation in the single and double-pass is given by the following simple equations:

$$AM_{\text{sp}}(\text{dB}) = 80.33 \cdot F^{-0.995} \quad (12)$$

$$AM_{dp}(\text{dB}) = 321.81 \cdot F^{-1.941}. \quad (13)$$

Setting $F = 50$ in (13), the amplitude modulation is calculated as 0.14 dB, a value that is almost identical to the one measured experimentally by the sampling oscilloscope and the microwave spectrum analyzer, which thus confirms the theory. Equations (12) and (13) show that, as far as the amplitude modulation is concerned, the filter finesse is effectively squared in the double pass configuration, even though the filter bandwidth is reduced only by $\sqrt{\sqrt{2}-1}$, as (6) indicates.

Equations (3) and (13) provide a design tool to calculate the necessary finesse of the FP filter so that the circuit at the output provides pulse trains at various repetition rates ($k = 2, 3, 4, \ldots$), under the condition that the amplitude modulation is restricted to a predefined value. Starting with an input pulse train at a 10-GHz repetition rate, the necessary finesse of the FP filter to achieve multiplication factors in the range of 2 to 16 with 0.14-dB amplitude modulation for the single- and double-pass arrangements has been plotted in Fig. 11. To obtain pulse trains at 160 GHz with the single-pass arrangement, the FP filter must have a finesse of 3000. If, however, the double-pass arrangement is used, then an FP filter with a finesse of 200 is adequate.

Given that FP filters operate over broad wavelength ranges are determined by their dielectric coatings, a single FP filter may be used to rate multiply a number of lower rate pulse trains coming from different laser diodes. As such, this technique may be applied in rate multiplication of several sources simultaneously for use in WDM experiments, sharing thus the already low cost between them and thus containing rate upgrade costs.

IV. Conclusion

We have presented two methods to achieve rate multiplication at various repetition rates. The first method employs an FP filter followed by an SOA and the second method uses a single FP filter in which the pulse train passes through twice. In comparison, the first method has the advantage of higher power at the expense of an active SOA element, while a $\times$ 16 multiplication factor might be hard to achieve with conventional SOAs. The second method has the advantage of simplicity and lower cost as well as easier multiplication to higher rates at the expense of output power. Both methods have been theoretically studied and experimentally verified for rate quadruplication from 10 to 40 GHz. The output pulse trains presented very low amplitude modulation and low jitter, while their waveforms remained stable for many hours under laboratory conditions. The circuits are relatively simple to implement and of low cost. In principle they could provide a solution to repetition rate upgrades of existing optical sources, without the need for their replacement or their driving electronics.

Acknowledgment

The authors would like to thank G. Guekos of ETHZ, R. Dall'Ara and S. Hansmann of Optospeed S.A. for the SOA, and W. Miller of Acterna for lending the SDH/STM 64 Network Analyzer.

References

[1] C. Wu and N. K. Dutta, "High-repetition-rate optical pulse generation using a rational harmonic mode-locked fiber laser," *IEEE J. Quantum Electron.*, pp. 145–150, Feb. 2000.

[2] Z. Li, C. Lou, K. T. Chan, Y. Li, and Y. Gao, "Theoretical and experimental study of pulse-amplitude-equalization in a rational harmonic mode-locked fiber ring laser," *IEEE J. Quantum Electron.*, vol. 37, pp. 33–37, Jan. 2001.

[3] W. W. Tang and C. Shu, "Optical generation of amplitude-equalized pulses from a rational harmonic mode-locked fiber laser incorporating an SOA loop modulator," *IEEE Photon. Technol. Lett.*, vol. 15, pp. 21–23, Jan. 2003.

[4] K. K. Gupta, N. Onodera, and M. Hyodo, "Technique to generate equal amplitude, higher-order optical pulses in rational harmonically mode-locked fiber ring lasers," *Elec. Lett.*, vol. 37, pp. 948–950, July 2001.

[5] Z. Ahmed and N. Onodera, "High repetition rate optical pulse generation by frequency multiplication in actively modelocked fiber ring laser," *Electron. Lett.*, vol. 32, pp. 455–457, Feb. 2001.

[6] K. Zoiros, K. Vlachos, T. Stathopoulos, C. Bintjas, and H. Avramoulos, "40 GHz mode-locked SOA fiber ring laser with 20 nm tuning range," in *Proc. Optical Fiber Communication Conf.*, 2000, TuR3, pp. 254–256.

[7] D. L. A. Seixas and M. C. R. Carvalho, "50 GHz fiber ring laser using rational harmonic mode-locking," in *Proc. Int. Conf. Microwave and Optoelectronics*, vol. 1, 2001, pp. 351–353.

[8] E. Yoshida and M. Nakazawa, "$80 \sim 200$ GHz erbium doped fiber laser using a rational harmonic mode-locking technique," *Electron. Lett.*, vol. 32, pp. 1370–1372, July 1996.

[9] H. Shi, G. Alphonse, J. Connolly, and P. Delfyett, "20×5 Gbit/s optical WDM transmitter using single-stripe multiwavelength modelocked semiconductor laser," *Electron. Lett.*, vol. 34, pp. 179–181, Jan. 1998.

[10] K. Vlachos, K. Zoiros, T. Houbavlis, and H. Avramopoulos, "10×30 GHz pulse train generation from semiconductor amplifier fiber ring laser," *IEEE Photon. Technol. Lett.*, vol. 12, pp. 25–27, Jan. 2000.

[11] L. Talaverano, S. Abad, S. Jarabo, and M. Lopez-Amo, "Multiwavelength fiber laser sources with Bragg-grating sensor multiplexing capability," *J. Lightwave Technol.*, vol. 19, pp. 553–558, Apr. 2001.

[12] J. Azana, R. Slavik, P. Kockaert, L. R. Chen, and S. LaRochelle, "Generation of ultra-high repetition rate optical pulse bursts by means of fiber Bragg gratings operating in transmission," *Electron. Lett.*, vol. 38, pp. 1555–1556, Nov. 2002.

[13] I. Shake, H. Takara, S. Kawanishi, and M. Saruwatari, "High-repetition-rate optical pulse generation by using chirped optical pulses," *Electron. Lett.*, vol. 34, pp. 792–793, Apr. 1998.

[14] S. Atkins and B. Fischer, "All-optical pulse rate multiplication using fractional Talbot effect and field-to- intensity conversion with cross-gain modulation," *IEEE Photon. Technol. Lett.*, vol. 15, pp. 132–134, Jan. 2003.

[15] D. E. Leaird, S. Shen, A. M. Weiner, A. Sugita, S. Kamei, M. Ishii, and K. Okamoto, "Generation of high-repetition-rate WDM pulse trains from an arrayed-waveguide grating," *IEEE Photon. Technol. Lett.*, vol. 13, pp. 221–223, Mar. 2001.

[16] N. K. Berger, B. Levit, S. Atkins, and B. Fischer, "Repetition-rate multiplication of optical pulses using uniform fiber Bragg gratings," *Opt. Commun.*, vol. 221, pp. 331–335, June 2003.

[17] T. Sizer, "Increase in laser repetition rate by spectral selection," *IEEE J. Quantum Electron.*, vol. 25, pp. 97–103, Jan. 1989.

[18] D. K. Serkland, G. D. Bartolini, W. L. Kath, P. Kumar, and A. V. Sahakian, "Rate multiplication of a 59-GHz soliton source at 1550 nm," *J. Lightwave Technol.*, vol. 16, pp. 670–677, Apr. 1998.

[19] K. K. Gupta *et al.*, "Pulse repetition frequency multiplication via intracavity optical filtering in AM mode-lockedfiber ring lasers," *IEEE Photon. Technol. Lett.*, vol. 14, pp. 284–286, Mar. 2002.

[20] M. Eiselt, W. Pieper, and H. G. Weber, "SLALOM: Semiconductor laser amplifier in a loop mirror," *J. Lightwave Technol.*, vol. 13, pp. 2099–2112, Oct. 1995.

[21] T. Akiyama *et al.*, "Nonlinear gain dynamics in quantum-dot optical amplifiers and its application to optical communication devices," *IEEE J. Quantum Elecrton.*, vol. 37, pp. 1059–1065, Aug. 2001.

[22] T. W. Berg, S. Bischoff, I. Magnusdottir, and J. Mork, "Ultrafast gain recovery and modulation limitations in self-assembled quantum-dot devices," *IEEE Photon. Technol. Lett.*, vol. 13, pp. 541–543, June 2001.

[23] M. Usami, M. Tsurusawa, and Y. Matsushima, "Mechanism for reducing recovery time of optical nonlinearity in semiconductor laser amplifier," *Appl. Phys. Lett.*, vol. 72, pp. 2657–2659, May 1998.

[24] R. J. Manning, D. A. O. Davies, S. Cotter, and J. K. Lucek, "Enhanced recovery rates in semiconductor laser amplifiers using optical pumping," *Electron. Lett.*, vol. 30, pp. 787–788, May 1994.

Konstantinos Yiannopoulos was born in Tripoli in December 1977. He received the Diploma of electrical engineering and computer science from the National Technical University of Athens, Athens, Greece, in 2000.

He has been with the Photonics Communications Research Laboratory, National Technical University of Athens, since 1999. His laboratory-related experience includes all-optical high-speed logic, optical signal processing for packet switched networks, and high-rate optical sources. He is the author or coauthor of more than ten papers in IEEE journals and sponsored conferences.

Mr. Yiannopoulos is a Student Member of the IEEE Lasers and Electro-Optics Society and the IEEE Communications Society.

Konstantinos Vyrsokinos was born in Thessaloniki, Greece, in 1977. He received the B.Sc. degree in physics from the Aristotle University of Thessaloniki, Thessaloniki, Greece, after carrying out his diploma thesis at the Technical University of Berlin in the frames of the ERASMUS exchange program. He is currently working toward the Ph.D. degree at the National Technical University of Athens, Athens, Greece.

His main interest was the application of gain clamped semiconductor optical amplifiers for fast all optical switching. From February until August 2001, he worked as a Laboratory Assistant at Heinrich-Hertz-Institut für Nachrichtentechnik Berlin GmbH, Berlin, Germany, in the optical signal processing group. Since January of 2002, he has been with the Photonics Communications Research Laboratory, National Technical University of Athens, performing his doctoral work. His fields of interest are optical signal processing for packet switched networks and high-speed optical sources. He is the author or coauthor of seven papers in IEEE journals and sponsored conferences.

Mr. Vyrsokinos is a Student Member of the IEEE Lasers and Electro-Optics Society.

Dimitris Tsiokos was born in Athens, Greece, in 1980. He received the B.Eng. degree in electronic engineering from the University of Southampton, Southampton, U.K., in 2001 and the M.Sc. degree in optics and photonics from Imperial College of Science Technology and Medicine, London, U.K., in 2002.

He has been with the Photonics Communications Research Laboratory of the National Technical University of Athens, Athens, Greece, since 2002. His laboratory-related work experience includes all-optical high-speed logic and optical signal processing for packet switched networks. He is the author or coauthor of six papers in IEEE journals and sponsored conferences.

He is a Student Member of the IEEE Lasers and Electro-Optics Society.

Efstratios Kehayas was born in Athens, Greece, in August 1980. He received the B.Eng. degree in electronic engineering from Southampton University, Southampton, U.K., and the M.Sc. degree in optics and photonics from Imperial College, London, U.K.

He has been with the Photonics Communications Research Laboratory, National Technical University of Athens, Athens, Greece, since 2002. His research field includes implementation of high-speed all-optical logic devices, photonic signal processing for packet switched networks, and optical sources. He is the author or coauthor of six publications in IEEE journals and sponsored conferences.

Mr. Kehayas is a Student Member of the IEEE Lasers and Electro-Optics Society.

N. Pleros was born in Athens, Greece, in September 1976. He received the Diploma of electrical and computer engineering from the National Technical University of Athens (NTUA), Athens, Greece, in 2000. He is currently working toward the Ph.D. degree in electrical and computer engineering.

His research interests include CW and mode-locked laser sources for high data-rate telecommunication applications, all-optical digital logic modules, all-optical packet/burst switching, and semiconductor-based switching devices. He is the author or coauthor of more than 20 publications.

Mr. Pleros was awarded one of the 12 fellowships provided within the international IEEE/LEOS Graduate Student Fellowship Program for the year 2003. In 1993, he was also awarded the 15th prize in the Greek Mathematical Olympiad in 1993. He is a Student Member of the IEEE Lasers and Electro-Optics Society and the Greek Technical Chamber.

George Theophilopoulos (M'04) was born in Athens, Greece in 1976. He received the Diploma of Electrical and Computer Engineering from the National Technical University of Athens (NTUA), Athens, Greece, in 1999 and the Ph.D. degree in electrical and computer engineering from the Photonics Communications Research Laboratory (PCRL), NTUA, in 2003.

Since then, he is a Senior Research Associate in PCRL. His research interests include all-optical logic, all-optical switches, optical networks and semiconductor switching technologies. He is the author or coauthor of 20 publications.

Thanassis Houbavlis was born in Athens, Greece, in November 1967. He received the Diploma of Physics with specialization in lasers from the University of Athens, Athens, Greece, in 1992, the M.Sc. degree in optoelectronics and laser devices from the Universities of Edinburgh and Saint Andrews, Scotland, in 1994, and the Ph.D. degree in optical communications from the Photonics Communications Research Laboratory, National Technical University of Athens, Athens, Greece, in 1999. His Ph.D. research focused on the design and implementation of ultrahigh-speed alloptical gates and subsystems.

He has participated in various European and national research projects. He is the author or coauthor of several articles in international technical journals and conferences.

Dr. Houbavlis is a Member of FITCE.

George Guekos (S'66–M'69) received the diploma in electrical engineering and the Ph.D. degree from the Swiss Federal Institute of Technology, ETH Zurich, Zurich, Switzerland.

He has been associated with the ETH since 1969, first as a Research Group Leader and Lecturer. He is now acting as a Professor teaching optoelectronics and fiber-optic communications and conducting research in optical waveguide structures. His interests include fabrication and characterization of photonic components like laser diodes, modulators and waveguide switches. He is actively involved in the European research network for the promotion of modern information technologies and he is engaged in the transfer of scientific research results to young companies.

Prof. Guekos is a Member of the Optical Society of America, the International Commission of Illumination CIE, the Swiss Optical Society, the Swiss Electrotechnical Society, and the Greek Society of Engineers.

Hercules Avramopoulos (M'91) received the B.S. degree in physics and the Ph.D. degree from the Imperial College of London, London, U.K.

He is currently heading the Photonics Technology Research Laboratory of the National Technical University of Athens (NTUA), Athens, Greece. From 1989 to 1993, he worked as a Member of Technical Staff in the Digital Optics Research Department, AT&T Bell Laboratories, Holmdel, NJ. His primary research interests have centered on the demonstration of novel concepts in photonic technologies for telecommunications. To this end he has worked on pulse generation, amplification, and transmission in optical fibers as well as on a large number of laser and amplifier systems for a variety of applications. For the past 10 years, he has worked and more recently he has supervised work on ultrahigh-speed, bitwise, all-optical, logic circuits and he has been interested to demonstrate their feasibility as a commercially viable technology for the telecommunications industry. He has been awarded four international patents in ultrahigh-speed switching systems and has more than 100 archival journal publications and presentations including several invited talks to major international conferences.

Mr. Avramopoulos is a Member of the IEEE Lasers and Electro-Optics Society.